NANO LETTERS

LETTER

pubs.acs.org/NanoLett

Silicon-Nanowire-Based CMOS-Compatible Field-Effect Transistor Nanosensors for Ultrasensitive Electrical Detection of Nucleic Acids

Anran Gao,[†,§] Na Lu,[‡,§] Pengfei Dai,[†] Tie Li,[*,†] Hao Pei,[‡] Xiuli Gao,[†] Yibin Gong,[†] Yuelin Wang,[†] and Chunhai Fan[*,‡]

[†]State Key Laboratories of Transducer Technology & Science and Technology on Micro-system Laboratory, Shanghai Institute of Microsystem and Information Technology, Chinese Academy of Sciences, Shanghai 200050, China

[‡]Laboratory of Physical Biology, Shanghai Institute of Applied Physics, Chinese Academy of Sciences, Shanghai 201800, China

Supporting Information

ABSTRACT: We herein report the design of a novel semiconducting silicon nanowire field-effect transistor (SiNW-FET) biosensor array for ultrasensitive label-free and real-time detection of nucleic acids. Highly responsive SiNWs with narrow sizes and high surface-to-volume-ratios were "top-down" fabricated with a complementary metal oxide semiconductor compatible anisotropic self-stop etching technique. When SiNWs were covalently modified with DNA probes, the nanosensor showed highly sensitive concentration-dependent conductance change in response to specific target DNA sequences. This SiNW-FET nanosensor revealed ultrahigh sensitivity for rapid and reliable detection of 1 fM of target DNA and high specificity single-nucleotide polymorphism discrimination. As a proof-of-concept for multiplex detection with this small-size and mass producible sensor array, we demonstrated simultaneous selective detection of two pathogenic strain virus DNA sequences (H1N1 and H5N1) of avian influenza.

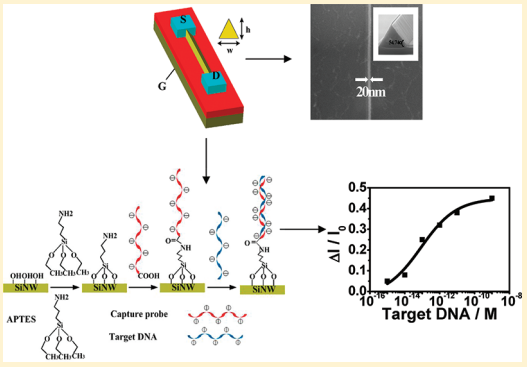

KEYWORDS: SiNW-FETs, biosensor, DNA detection, label-free, ultrasensitive

One-dimensional nanostructures have proven to be promising candidates for recognizing a wide range of biological and chemical species.[1] Semiconducting silicon nanowire (SiNW) based field-effect transistors (FETs) have exhibited high sensitivity and multiplex capability to detect specific receptor molecules.[2] The high sensitivity of the SiNW-type nanosensors arises due to their small size and large surface-to-volume ratio.[3] Consequently, conductance of SiNW changes remarkably upon the binding of even a small quantity of charged molecules. By exploiting this attractive property, a variety of SiNW-FET nanosensor devices have been designed for the detection of various targets including DNA,[4] proteins,[5−7] small molecules,[8] metal ions and chemical species,[6,9,10] single virus particles,[11] and even cells.[12] In this work, we report the fabrication of highly responsive SiNW array with homogeneous narrow sizes and high aspect ratios by using a complementary metal oxide semiconductor (CMOS) compatible anisotropic wet etching approach with self-stop limitation. The nanosensor array employing such SiNWs revealed ultrahigh sensitivity for rapid and reliable detection of target DNA as low as 1 fM and high specificity for single-nucleotide polymorphism (SNP) discrimination.

In nanoelectronics, SiNWs can be fabricated either "bottom-up" or "top-down". The "bottom-up" approach[13] relies on the assembly of grown SiNWs, which nevertheless inherently suffers from the limitations of complex integration. More recently, the alternative top-down approach[14−16] has attracted great interest due to its mass manufacturing ability and potential compatibility with the conventional silicon industry.[5,17−19] Significantly, Reed and co-workers developed an anisotropic wet etch process technology with CMOS compatibility to fabricate SiNWs, which formed the basis for label-free immunodetection of sub-100 fM immunoglobulins G and A.[5]

Results and Discussion. The sensitivity of SiNW-type FET nanosensors is critically dependent on the size of SiNWs.[3] In order to fabricate SiNWs with narrow sizes and high aspect ratios, we developed an anisotropic wet etch employing a self-stop limitation which is compatible with current commercial semiconductor processes. Conventional optical lithography[20] was combined with anisotropic wet etching with tetramethylammonium hydroxide (TMAH). TMAH anisotropically etched silicon (Si) with slower etching speed of Si(111) plane than other planes, hence leading to slow degradation from the bulk silicon, an effect that overcomes the limitations of traditional manufacturing methods.[21] Since dry oxidation of silicon down to the nanometer level is a self-limiting process[22,23] and Si(111) etch rate was slower than other planes, the size of silicon structures is highly controllable and reproducible. By controlling etching time and the self-limiting oxidation, we obtained homogeneous arrays

Received: July 6, 2011
Revised: August 9, 2011
Published: August 17, 2011

dx.doi.org/10.1021/nl202303y | *Nano Lett.* 2011, 11, 3974–3978

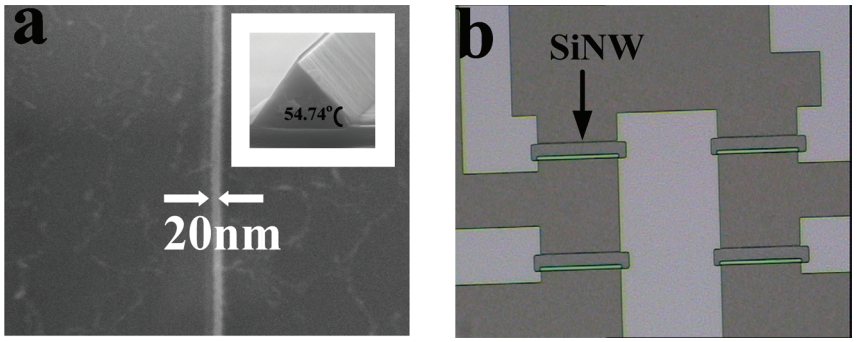

Figure 1. SiNW fabrication and SiNW array. (a) A representative scanning electron microscopy image of a SiNW with the width less than 20 nm. The inset shows a cross-sectional view of fabricated nanowire. An angle of 54.74° with Si(100) top and bottom surfaces were formed. (b) Optical micrograph of a quarter of a completed SiNW array. Four individual SiNWs are aligned and separated by 70 μm spacing.

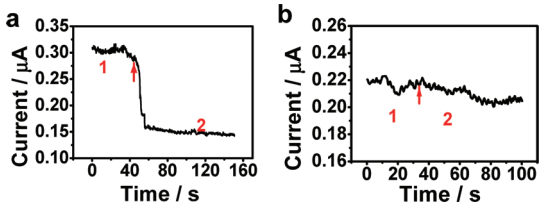

Figure 2. Plots of current versus time for the SiNW-FET DNA sensor (a) and the unmodified SiNW-FET (b), where region 1 stands for the flow of buffer solution and region 2 for the addition of 1 nM of fully cDNA. The SiNW devices used in (a) and (b) were both n-type and phosphorus-doped nanowires, with length of 6 μm.

of SiNW of the triangular cross section, with high surface-to-volume ratios and controllable sizes ranging from 20 to 200 nm.

We fabricated a SiNW-FET device (shown in Figure S2a, Supporting Information) by using commercially available (100) silicon-on-insulator (SOI) wafers and anisotropic TMAH etching. During the fabrication process, Si_3N_4 acted as sidewall protection layers and SiO_2 as masks for Si(111) planes, and TMAH anisotropic etching was a crucial step that decided the cross-sectional shape of the SiNWs (Figure S1, Supporting Information). We obtained smooth, triangular SiNW structures with Si(111) sidewalls at an angle of 54.74° with (100) top and bottom surfaces (Figure 1a, inset). The fabricated SiNWs with single crystalline structure had large surface-to-volume ratio, and the triangular shape was beneficial for obtaining narrow SiNWs. Owing to the planarization of the anisotropic wet etching, the surface of SiNWs was fairly smooth.

The width of the SiNW in the lateral direction was linearly proportional with the etching time with the lateral etching rate of ~2.3 nm/min (Figure S3, Supporting Information). Hence, the width of SiNW could be precisely controlled by varying the etching time. By finely controlling the etching time and thermal oxidization, we could narrow the diameter of nanowires down to 20 nm, as visualized in a scanning electron micrograph (SEM, Figure 1a). It was no other than the triangular shape to give rise to the so small size of SiNW. Moreover, the fabricated nanowires also have well-distributed sizes and uniform conductance in statistics (Figure S4, Supporting Information). The fabricated arrays contain 16 uniform and well-aligned SiNWs of both p-type and n-type (Figure 2b). The incorporation of both p-type and n-type nanowires in a single chip allows effective discrimination of possible electrical cross-talk and false-positive signals by correlating the response versus time from the two types of device elements (see also Figure S8, Supporting Information).[2] Optical microscopic observation confirmed that the aligned SiNWs were uniform and well-ordered (Figure 1b). These studies showed that the CMOS-compatible sensor array could be conveniently fabricated with high controllability, reproducibility, and throughput.

A prototype FET device was fabricated with the SiNW array (see Figure S5a of the Supporting Information). The SiNW-FET devices demonstrated excellent electrical properties, as shown in parts b and c of Figure S5 in the Supporting Information. Particularly, we observed almost no electronic hysteresis, suggesting the presence of a low density of trapped charges inside the structure. Previous work suggested that TMAH-etched electronic devices, despite their good electrical properties, were often not suitable for sensing charged molecules.[24] However, it is interesting that our SiNW-FETs rapidly and sensitively responded to the pH change of the solution when SiNWs were silanized at the exposed, dominant Si(111) planes which is preferred for selective surface functionalization (Figure S6 of the Supporting Information),[25] suggesting that this device is particularly appropriate for sensing.

We then employed the n-type SiNW-FET device to electrically detect DNA hybridization. Capture probe DNA with the terminal carboxyl group was conjugated to the amine of the (3-aminopropyl)triethoxysilane (APTES)-modified SiNWs, with the help of *N*-hydroxysuccinimide (NHS) and 1-ethyl-3-(3-dimethylaminopropyl)carbodiimide (EDC) (Figure S7, Supporting Information).[26,27] When the buffer solution was flowed through the sensor surface, the electrical response of the SiNW-FET remained nearly unchanged (Figure 2a). Significantly, when a solution containing 1 nM of fully complementary target DNA was introduced, we observed a rapid decrease of the electrical current down to nearly half of the initial value within seconds. Of note, the hybridization process could be monitored in real time with this SiNW-FET sensor. The decrease in electrical current coincides well with previous reports,[4,5] suggesting that the binding of negatively charged target DNA to the gate dielectric of n-type SiNW-FET results in the depletion of carriers[28,29] As a control experiment, target DNA of the same concentration was flowed through an unmodified SiNW FET, which did not lead to significant current change (Figure 2b), suggesting the absence of nonspecific binding of target DNA to the SiNW surface.

The sensitivity of the SiNW-FET sensor was interrogated by challenging it with a series of concentrations of target DNA.

dx.doi.org/10.1021/nl202303y |*Nano Lett.* 2011, 11, 3974–3978

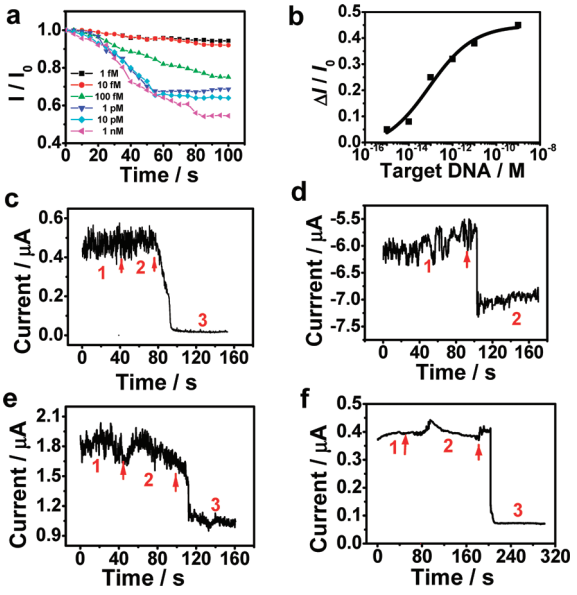

Figure 3. Real-time detection of target DNA with the SiNW-FET sensor. (a) Plots of normalized current change versus time with target DNA at a series of concentrations (1 fM, 10 fM, 100 fM, 1 pM, 10 pM, and 1 nM) for probe DNA modified SiNW device. (b) Normalized current change ($|I/I_0|$) as a function of the logarithm of target DNA concentration. I represents the value of the final current (t = 100 s), and I_0 represents the value of the initial current (t = 0). (c, d) Evaluation of the specificity of the SiNW-FET sensor. Plots of current versus time for probe DNA modified SiNWs. (c) Region 1 corresponds to buffer solution, region 2 corresponds to the addition of 100 nM noncDNA, and region 3 corresponds to the addition of 100 nM fully cDNA. The nanowires used were n-type, phosphorus doped. (d) Region 1 corresponds to buffer solution, and region 2 corresponds to the addition of 1 μM of one-base mismatched DNA. p-type and boron-doped SiNWs were used. (e, f) Simultaneous detection of two high pathogenic strain viruses DNA. (e) Plot of current versus time for $H1N1_{probe}$ DNA modified SiNWs, where region 1 corresponds to buffer solution, region 2 corresponds to the addition of 10 nM of $H5N1_{target}$ DNA, and region 3 corresponds to the introduction of 10 nM of $H1N1_{target}$ DNA. (f) Real-time current responses from a SiNW device functionalized with $H5N1_{probe}$ DNA, during flow of free buffer (1), 10 nM of $H1N1_{target}$ DNA (2), and 10 nM of $H5N1_{target}$ DNA (3). Arrows mark the points when the solutions were introduced. The nanowires used in (e) and (f) were both of n-type and phosphorus doped. The length of SiNWs used in these studies was of 6 μm.

The data were normalized by computing $|I/I_0|$[7] and plotted on the same axes for the change in current of the SiNW device, as shown in Figure 3a. Here, I represents the value of the final current (t = 100 s), and I_0 represents the value of the initial current (t = 0).We found that the nanosensor could reliably detect target DNA down to a concentration as low as 1 fM. This sensitivity is higher than the previously reported SiNW-FET nanosensor,[5] possibly due to the use of SiNWs with small sizes. The use of peptide nucleic acids (PNA) as receptors[4] might further increase the sensitivity since PNA probes possess higher affinity to DNA targets than DNA probes.

A calibration curve for the DNA detection was provided in Figure 3b. Here, we define a relative suppression ratio of the current for the response of the device to the target DNA: $\Delta I/I_0$, where ΔI is the change of the current in the assay. The electrical current change increased monotonously with the logarithm of DNA concentration. The ability to detect 1 fM of target DNA implies the ultrahigh sensitivity of this SiNW-FET sensor. We further evaluated the specificity of the SiNW-FET sensor. Figure 3c confirms that noncognate DNA of 100 nM did not lead to significant change of the electrical current, which was in sharp contrast with the addition of 100 nM of target DNA. As shown in Figure 3d, the introduction of a one-base mismatched DNA only led to current change of ~20%, which was significantly lower than that for 1 nM of fully complementary target DNA (nearly 50%). This suggests that the SiNW-FET sensor possesses one-base mismatch discrimination ability for single-nucleotide polymorphism (SNP) detection.

Given the high specificity of the SiNW-FET sensor, we employed it to simultaneously detect two virus DNA sequences (H1N1 and H5N1) associated with avian influenza. Avian influenza is well-known to be highly pathogenic and has different subtypes including H1N1 and H5N1. Two probe DNA, $H1N1_{probe}$ and $H5N1_{probe}$, were immobilized on the surface of two SiNWs, respectively. Significantly, the electrical responses of the functionalized SiNW-FETs were selectively dependent on the presence of different targets ($H1N1_{target}$ and $H5N1_{target}$). That is, the $H1N1_{probe}$ functionalized SiNW only led to significant decrease in current in the presence of $H1N1_{target}$, while not $H5N1_{target}$ (Figure 3e). Similar results were obtained for the $H5N1_{probe}$ functionalized SiNW (Figure 3f).

Conclusions. We have developed a CMOS-compatible anisotropic wet etching technique for the fabrication of SiNW arrays and high-performance SiNW-FET device. This device allows electrical sensing in real time, and multiplexing is possible due to the presence of 16 individually aligned SiNWs. We have demonstrated that this nanosensor can rapidly and sensitively detect as low as 1 fM DNA, with the high specificity for one-base mismatch discrimination. This extremely high sensitivity excels most previously reported DNA sensors with various transducers.[30−40] As a proof-of-concept for multiplex detection, we have realized simultaneous detection of two pathogenic virus DNA sequences. Given the extraordinary ability for real-time and label-free biomolecular detection, and the small size and low cost of mass producible CMOS-compatible devices, we expect it will provide a generic platform for numerous applications including point-of-care test.

Experimental Section. *Materials and Reagents.* (3-Aminopropyl)triethoxysilane (APTES), 1-ethyl-3-(3-(dimethylaminopropyl) carbodiimide (EDC), and *N*-hydroxysuccinimide (NHS) were purchased from Sigma-Aldrich (USA) and used as received. Other chemicals were obtained from Sinopharm Chemical Reagent Co., Ltd. (Shanghai, China). All solutions were prepared with Milli-Q water (18 MΩ·cm, Millipore) from a Millipore system.

Nucleic Acids Sequences. All oligonucleotides with the following sequences were custom-synthesized and purified by Shanghai Sangon Bioengineering Technology and Services Co., Ltd. (Shanghai, China): capture probe, 5′-HOOC-CAC GAC GTT GTA AAA CGA CGG CCA G-3′; fully complementary target, 5′-CTG GCC GTC GTT TTA CAA CGT CGT G-3′; one-base mismatched DNA (italic base indicates the mismatched one), 5′-CTG GCC GTC GTT *CTA* CAA CGT CGT G-3′; NoncDNA, 5′-TGA TAA CCA ATG CAG ATT TTG AGC A-3′; AIV H1N1 probe, 5′-HOOC-CAC ACT CTG TCA ACC TAC-3′; AIV H1N1 target, 5′-GTA GGT TGA CAG AGT GTG-3′; AIV H5N1 probe, 5′-HOOC-CAA ATC TGC ATT GGT TAT CA-3′; AIV H5N1 target, 5′-TGA TAA CCA ATG CAG ATT TG-3′.

Fabrication of SiNW Arrays. Commercially available (100) oriented SIMOX silicon-on-insulator (SOI) wafers with light boron adulteration of 5×10^{15} cm^{-3} were used in this method.

dx.doi.org/10.1021/nl202303y |*Nano Lett.* 2011, 11, 3974–3978

By employing TMAH, the boundary of the top silicon layer was automatically aligned to the ⟨110⟩ direction and a very smooth (111) plane formed beneath the SiO_2 mask (Figure S1a, Supporting Information). Then a thin nitride film (50 nm) was deposited by low-pressure chemical vapor deposition (LPCVD) to protect the (111) plane previously defined (Figure S1b, Supporting Information). After the nitride film was patterned by ion-beam etching, the 100 nm SiO_2 layer beneath was totally removed by diluted HF (Figure S1c, Supporting Information). Then by using TMAH for the second time, we obtained controllable SiNW arrays with a triangular cross section after removing the nitride film (Figure S1d, Supporting Information). Next, a high-quality SiO_2 layer with a thickness of 30 nm was thermally oxidized on the silicon nanowire surfaces (Figure S1e, Supporting Information), and then Si_3N_4 was removed by phosphoric acid at 150 °C (Figure S1f, Supporting Information). Finally, the nanowire was further etched by TMAH and even narrower SiNW was obtained (Figure S1g, Supporting Information). Figure S1h (Supporting Information) shows the fabricated SiNW with a triangular cross section and with single side silicon oxide as protection after removing the nitride film in Figure S1f (Supporting Information).

Surface Modification. The SiNW array was first cleaned in a piranha solution at 90 °C and then was functionalized by exposing the surface to APTES solution (2% ethanol) overnight. Finally, 1 μM 5′-carboxyl-modified single-stranded DNA (ssDNA) in phosphate buffered saline (PBS, 137 mM NaCl, 2.7 mM KCl, and 10 mM phosphate, pH 7.4) was coupled to the surface of the nanowire for 2 h, followed by thoroughly washing with the same buffer and Milli-Q water (18 MΩ·cm, Millipore).

DNA Sensing. For DNA sensing, the measurements were performed by using a Keithley 4200 semiconductor parameter analyzer (Keithley Instruments Inc., Cleveland, OH). All devices used for functionalized-sensing experiments were similar, with w = 200 nm approximately. For sensing measurements, we used V_{DS} = +1 V, V_{GS} = +10 V for n-type SiNWs and V_{DS} = −1 V, V_{GS} = −12 V for p-type SiNWs, respectively. Each measurement was carried out on a distinct device. All solutions used in hybridization studies were 0.1 ×PBS, in which Debye length is sufficiently long to ensure effective sensing during the capture process.[41]

■ ASSOCIATED CONTENT

Ⓢ Supporting Information. Fabrication of SiNW arrays, electrical measurements, SiNW FETs surface modification, and pH sensing. This material is available free of charge via the Internet at http://pubs.acs.org.

■ AUTHOR INFORMATION

Corresponding Author

*E-mail: tli@mail.sim.ac.cn (T. Li); fchh@sinap.ac.cn (C. Fan).

Author Contributions

§These authors contributed equally to this work.

■ ACKNOWLEDGMENT

The first two authors, A. Gao and N. Lu, contributed equally to this work. We appreciate financial support from National Basic Research Program of China (973 Program 2011CB309501, 2012CB932600), Creative Research of National Natural Science Foundation of China (61021064), and the National Natural Science Foundation of China (60936001, 60876037, 20725516, 20873175, 90913014).

■ REFERENCES

(1) Xia, Y.; Yang, P.; Sun, Y.; Wu, Y.; Mayers, B.; Gates, B.; Yin, Y.; Kim, F.; Yan, H. One-Dimensional Nanostructures: Synthesis, Characterization, and Applications. *Adv. Mater.* **2003**, *15*, 353–389.

(2) Zheng, G.; Patolsky, F.; Cui, Y.; Wang, W. U.; Lieber, C. M. Multiplexed Electrical Detection of Cancer Markers with Nanowire Sensor Arrays. *Nat. Biotechnol.* **2005**, *23*, 1294–1301.

(3) Elfström, N.; Juhasz, R.; Sychugov, I.; Engfeldt, T.; Karlström, A. E.; Linnros, J. Surface Charge Sensitivity of Silicon Nanowires: Size Dependence. *Nano Lett.* **2007**, *7*, 2608–2612.

(4) Hahm, J.-i.; Lieber, C. M. Direct Ultrasensitive Electrical Detection of DNA and DNA Sequence Variations Using Nanowire Nanosensors. *Nano Lett.* **2004**, *4*, 51–54.

(5) Stern, E.; Klemic, J. F.; Routenberg, D. A.; Wyrembak, P. N.; Turner-Evans, D. B.; Hamilton, A. D.; LaVan, D. A.; Fahmy, T. M.; Reed, M. A. Label-Free Immunodetection with CMOS-Compatible Semiconducting Nanowires. *Nature* **2007**, *445*, 519–522.

(6) Cui, Y.; Wei, Q.; Park, H.; Lieber, C. M. Nanowire Nanosensors for Highly Sensitive and Selective Detection of Biological and Chemical Species. *Science* **2001**, *293*, 1289–1292.

(7) Chua, J. H.; Chee, R.-E.; Agarwal, A.; Wong, S. M.; Zhang, G.-J. Label-Free Electrical Detection of Cardiac Biomarker with Complementary Metal-Oxide Semiconductor-Compatible Silicon Nanowire Sensor Arrays. *Anal. Chem.* **2009**, *81*, 6266–6271.

(8) Wang, W. U.; Chen, C.; Lin, K.-h.; Fang, Y.; Lieber, C. M. Label-Free Detection of Small-Molecule-Protein Interactions by Using Nanowire Nanosensors. *Proc. Natl. Acad. Sci. U.S.A.* **2005**, *102*, 3208–3212.

(9) Luo, L.; Jie, J.; Zhang, W.; He, Z.; Wang, J.; Yuan, G.; Zhang, W.; Wu, L. C. M.; Lee, S.-T. Silicon Nanowire Sensors for Hg^{2+} and Cd^{2+} ions. *Appl. Phys. Lett.* **2009**, *94*, 193101.

(10) McAlpine, M. C.; Ahmad, H.; Wang, D.; Heath, J. R. Highly Ordered Nanowire Arrays on Plastic Substrates for Ultrasensitive Flexible Chemical Sensors. *Nat. Mater.* **2007**, *6*, 379–384.

(11) Patolsky, F.; Zheng, G.; Hayden, O.; Lakadamyali, M.; Zhuang, X.; Lieber, C. M. Electrical Detection of Single Viruses. *Proc. Natl. Acad. Sci. U.S.A.* **2004**, *101*, 14017–14022.

(12) Stern, E.; Steenblock, E. R.; Reed, M. A.; Fahmy, T. M. Label-Free Electronic Detection of the Antigen-Specific T-Cell Immune Response. *Nano Lett.* **2008**, *8*, 3310–3314.

(13) Huang, Y.; Duan, X.; Wei, Q.; Lieber, C. M. Directed Assembly of One-Dimensional Nanostructures into Functional Networks. *Science* **2001**, *291*, 630–633.

(14) Elibol, O. H.; Morisette, D.; Akin, D.; Denton, J. P.; Bashir, R. Integrated Nanoscale Silicon Sensors Using Top-Down Fabrication. *Appl. Phys. Lett.* **2003**, *83*, 4613–4615.

(15) Kim, A.; Ah, C. S.; Yu, H. Y.; Yang, J.-H.; Baek, I.-B.; Ahn, C.-G.; Park, C. W.; Jun, M. S. Ultrasensitive, Label-Free, and Real-Time Immunodetection Using Silicon Field-Effect Transistors. *Appl. Phys. Lett.* **2007**, *91*, 103901.

(16) Li, Z.; Chen, Y.; Li, X.; Kamins, T. I.; Nauka, K.; Williams, R. S. Sequence-Specific Label-Free DNA Sensors Based on Silicon Nanowires. *Nano Lett.* **2004**, *4*, 245–247.

(17) Agarwal, A.; Buddharaju, K.; Lao, I. K.; Singh, N.; Balasubramanian, N.; Kwong, D. L. Silicon Nanowire Sensor Array Using Top-Down CMOS Technology. *Sens. Actuators, A* **2008**, *145−146*, 207–213.

(18) Pui, T.-S.; Agarwal, A.; Ye, F.; Balasubramanian, N.; Chen, P. CMOS-Compatible Nanowire Sensor Arrays for Detection of Cellular Bioelectricity. *Small* **2009**, *5*, 208–212.

(19) Pui, T.-S.; Agarwal, A.; Ye, F.; Tou, Z.-Q.; Huang, Y.; Chen, P. Ultra-Sensitive Detection of Adipocytokines with CMOS-Compatible Silicon Nanowire Arrays. *Nanoscale* **2009**, *1*, 159–163.

(20) Guo, L.; Krauss, P. R.; Chou, S. Y. Nanoscale Silicon Field Effect Transistors Fabricated Using Imprint Lithography. *Appl. Phys. Lett.* **1997**, *71*, 1881–1883.
(21) Tabata, O.; Asahi, R.; Funabashi, H.; Shimaoka, K.; Sugiyama, S. Anisotropic Etching of Silicon in TMAH Solutions. *Sens. Actuators, A* **1992**, *34*, 51–57.
(22) Grydlik, M.; Brehm, M.; Hackl, F.; Groiss, H.; Fromherz, T.; Schäffler, F.; Bauer, G. Inverted Ge Islands in {111} Faceted Si Pits-A Novel Approach towards SiGe Islands with Higher Aspect Ratio. *New J. Phys.* **2010**, *12*, 063002.
(23) Sievilä, P.; Chekurov, N.; Tittonen, I. The Fabrication of Silicon Nanostructures by Focused-Ion-Beam Implantation and TMAH Wet Etching. *Nanotechnology* **2010**, *21*, 145301.
(24) Liu, Y.; Ishii, K.; Tsutsumi, T.; Masahara, M.; Suzuki, E. Ideal Rectangular Cross-Section Si-Fin Channel Double-Gate MOSFETs Fabricated Using Orientation-Dependent Wet Etching. *IEEE Electron Device Lett.* **2003**, *24*, 484–486.
(25) Bunimovich, Y. L.; Ge, G.; Beverly, K. C.; Ries, R. S.; Hood, L.; Heath, J. R. Electrochemically Programmed, Spatially Selective Biofunctionalization of Silicon Wires. *Langmuir* **2004**, *20*, 10630–10638.
(26) Beier, M.; Hoheisel, J. D. Versatile Derivatisation of Solid Support Media for Covalent bonding on DNA-Microchips. *Nucleic Acids Res.* **1999**, *27*, 1970–1977.
(27) Li, Z.; Rajendran, B.; Kamins, T. I.; Li, X.; Chen, Y.; Williams, R. S. Silicon Nanowires for Sequence-Specific DNA Sensing: Device Fabrication and Simulation. *Appl. Phys. A: Mater. Sci. Process.* **2005**, *80*, 1257–1263.
(28) Bergveld, P. *IEEE Trans. Biomed. Eng.* **1972**, *BME-19*, 342.
(29) Blackburn, G. F. In *Biosensors: Fundamentals and Applications*; Turner, A. P. F., Karube, I., Wilson, G. S., Eds.; Oxford University Press: Oxford, 1987; pp 481−530.
(30) Fan, C.; Plaxco, K. W.; Heeger, A. J. Electrochemical Interrogation of Conformational Changes as A Reagentless Method for The Sequence-Specific Detection of DNA. *Proc. Natl. Acad. Sci. U.S.A.* **2003**, *100*, 9134–9137.
(31) Li, D.; Song, S.; Fan, C. Target-Responsive Structural Switching for Nucleic Acid-Based Sensors. *Acc. Chem. Res.* **2010**, *43*, 631–641.
(32) Song, S.; Qin, Y.; He, Y.; Huang, Q.; Fan, C.; Chen, H.-Y. Functional Nanoprobes for Ultrasensitive Detection of Biomolecules. *Chem. Soc. Rev.* **2010**, *39*, 4234–4243.
(33) Huang, Y.; Chen, P. Nanoelectronic Biosensing of Dynamic Cellular Activities Based on Nanostructured Materials. *Adv. Mater.* **2010**, *22*, 2818–2823.
(34) Zhang, J.; Song, S.; Zhang, L.; Wang, L.; Wu, H.; Pan, D.; Fan, C. Sequence-Specific Detection of Femtomolar DNA via a Chronocoulometric DNA Sensor (CDS): Effects of Nanoparticle-Mediated Amplification and Nanoscale Control of DNA Assembly at Electrodes. *J. Am. Chem. Soc.* **2006**, *128*, 8575–8580.
(35) He, S.; Song, B.; Li, D.; Zhu, C.; Qi, W.; Wen, Y.; Wang, L.; Song, S.; Fang, H.; Fan, C. A Graphene Nanoprobe for Rapid, Sensitive, and Multicolor Fluorescent DNA Analysis. *Adv. Funct. Mater.* **2010**, *20*, 453–459.
(36) Hansen, J. A.; Mukhopadhyay, R.; Hansen, J. Ø.; Gothelf, K. V. Femtomolar Electrochemical Detection of DNA Targets Using Metal Sulfide Nanoparticles. *J. Am. Chem. Soc.* **2006**, *128*, 3860–3861.
(37) Tyagi, S.; Bratu, D. P.; Kramer, F. R. Multicolor Molecular Beacons for Allele Discrimination. *Nat. Biotechnol.* **1998**, *16*, 49–53.
(38) Park, S. J.; Taton, T. A.; Mirkin, C. A. Array-Based Electrical Detection of DNA with Nanoparticle Probes. *Science* **2002**, *295*, 1503–1506.
(39) Xiao, Y.; Pavlov, V.; Niazov, T.; Dishon, A.; Kotler, M.; Willner, I. Catalytic Beacons for the Detection of DNA and Telomerase Activity. *J. Am. Chem. Soc.* **2004**, *126*, 7430–7431.
(40) Tian, Y.; He, Y.; Mao, C. Cascade Signal Amplification for DNA Detection. *ChemBioChem* **2006**, *7*, 1862–1864.
(41) Stern, E.; Wagner, R.; Sigworth, F. J.; Breaker, R.; Fahmy, T. M.; Reed, M. A. Importance of the Debye Screening Length on Nanowire Field Effect Transistor Sensors. *Nano Lett.* **2007**, *7*, 3405–3409.